Simplified Model of a Continuous Wave Diffusion-Type Chemical Laser – An Extension

Harold Mirels*
The Aerospace Corporation, El Segundo, Calif.

The simplified two-vibrational-level model of a cw diffusion-type chemical laser presented by Mirels, Hofland, and King is extended to include multiple vibrational levels. Both laminar and turbulent diffusion are considered. Expressions for axial gain distribution and net output power from a Fabry-Perot optical resonator are deduced. For a given lasing species, the resulting cw chemical laser scaling laws are the same as those previously deduced by Mirels, Hofland, and King, except for the dependence of certain coefficients on rotational quantum number J and temperature T. Broadwell previously presented a multiple-vibrational-level model for a cw chemical laser that was limited, however, to turbulent diffusion. The flame-sheet-mixing model used in the present study is shown to give results that are identical with those from the scheduled-mixing model of Broadwell when mean chemical rates are used.

Nomenclature

$A, A_v, A_{v,J}$ = $e^{-2JT_R/T}$
a_v = fraction on particles pumped into level v, $k_p^{(v)}/k_p$
C_1, C_2, C_3 = functions of JT_R/T, Eq. (25)
F_v = defines N_v in saturated oscillator, Eq. (22)
G_c = normalized gain/semichannel in optical cavity, $\sigma_v G_v/\sigma_0$
G_v = normalized gain per semichannel, Eq. (4)
$g_v, g_{v,J}$ = gain per unit length on transition $v+1, J-1 \rightarrow v, J$, cm^{-1}
H_v = defines effect on N_v of $G_c \neq 0$, Eq. (22)
ΔH = net energy (J) released by pumping reaction/mole of n_r
$\bar{I}_v, \bar{I}_{v,J}$ = local lasing intensity, W/cm^2
$I_v, I_{v,J}$ = normalized value of lasing intensity, Eq. (4)
J = rotational quantum number
K_1 = ratio of net pumping rate to $v=1 \rightarrow v=0$ deactivation rate, $k_p/k_{cd}^{(1)}$
k = mean rate, sec^{-1}
$\bar{k}$ = rate coefficient, cm^3/(mol-sec)
M = molecular weight of excited species
m = 1 for laminar and turbulent flames, respectively
N_{ToT} = measure of net number of particles in levels $v=0$ to $v=v_f$ at station x
N_i = measure of net amount of species i at station x, Eq. (4)
n_i = local number density of species i, mol/cm^3
n_r = reference number density {equals $[n_F]_\infty$ for cold reaction HF (DF) lasers}
n_{sc} = number of semichannels
P = net output power/semichannel, emitted up to station x, W/cm
P_e = net oscillator output power/semichannel, W/cm
R_1, R_2 = reflectivity of mirrors 1 and 2
r_v = relative deactivation rate, $[k_{cd}^{(v)} + k_{sp}^{(v)}]/k_{cd}^{(1)}$
T = rotational and translational temperature, °K
T_R = characteristic rotational temperature, °K
u = flow velocity in x direction, cm/sec
v = vibrational level, $v = 0, 1, \ldots, v_f$
v_f = highest vibrational level considered
w = oxidizer channel semiwidth, cm (Fig. 1)
x = axial distance, cm
x_D = characteristic diffusion distance, $y_f(x_D) = w$
x_o = flame sheet abscissa, cm
Y = $y_f(x)/w$
Y_o = $y_f(x_o)/w$
$y_f(x)$ = flame sheet ordinate, cm
ϵ = mean value of ϵ_v
ϵ_v = energy (joules)/mol of photons for transition $v+1, J-1 \rightarrow v, J$
ϕ = net photon output up to station ζ, per initial reference (n_r) particle, $\phi = \sum_{v=0}^{v_f-1} \phi_v$
ϕ_v = value of ϕ for single transition $v+1, J-1 \rightarrow v, J$
ϕ_e = net photon output/initial n_r particle for an oscillator
ζ = normalized axial distance, $k_{cd}^{(1)} x/u$
ζ_D = ratio of characteristic diffusion distance to characteristic deactivation distance, $k_{cd}^{(1)} x_D/u$
ζ_e = value of ζ at end of lasing zone in oscillator
ζ_i = value of ζ at which lasing is initiated
$\sigma_v, \sigma_{v,J}$ = cross section for stimulated emission, Eq. (2), cm^2/mol
η_c = chemical efficiency, Eq. (26)

Subscripts

cd = collisional deactivation
F, F_2 = atomic or molecular fluorine, respectively
i = species i
p = pumping reaction
sp = spontaneous emission
v = vibrational energy level
v or v,J = associated with transition $v+1, J-1 \rightarrow v, J$

Received July 24, 1975; revision received Dec. 15, 1975. This work reflects research supported by the Air Force Space and Missile Systems Organization (SAMSO) under Contract F04701-74-C-0075.
Index categories: Lasers; Reactive Flows.
*Head, Aerodynamics and Heat Transfer Department, Laboratory Operations. Fellow AIAA.

∞ = freestream value
0 = corresponding to $v=0$ or x_o

I. Introduction

VARIOUS approaches have been taken to analyze the performance of cw diffusion-type HF/DF chemical lasers theoretically. These include the development of computer programs that use boundary-layer approximations in the mixing region,[1-3] an "exact" analytical flame-sheet solution for laminar mixing in the limit of zero power[4] or optical saturation,[5] and solutions in which simplified mixing and chemical kinetics models are used.[6,7] The latter do not satisfy the equations of motion, even in a limiting sense, but do describe the basic behavior of the cw diffusion-type chemical laser in terms of relevant normalized parameters.

A flame-sheet diffusion model was used by Mirels, Hofland, and King.[6] Laminar and turbulent mixing were analyzed, as well as oscillator and amplifier configurations. To obtain simple closed-form solutions, a two-level vibrational model was used.

Broadwell[7] extended the analysis of Emanuel and Whittier[8] to include effects of diffusion on HF laser performance. A scheduled-mixing model was used; turbulent mixing and an oscillator optical configuration were assumed; multiple vibrational levels were considered.

In the present study, the analysis of Mirels, Hofland, and King[6] is extended to include multiple vibrational levels. Arbitrary mixing rates and chemical rate coefficients are considered. Solutions for zero power and amplifier cases, as well as expressions for total oscillator output power, are obtained. In addition, the flame-sheet[6] and the scheduled-mixing[7] models are compared.

II. Theory

In the following sections, the rate of formation and deactivation of excited species in a cw diffusion-type chemical laser is discussed. Equations that describe the performance of amplifier or oscillator configurations are then noted.

A. Basic Equations

The mixing model of Mirels, Hofland, and King[6] is illustrated in Fig. 1. The flow downstream of a single oxidizer (F) semichannel is considered. The reactants are assumed to be premixed, but do not start to react until a specified flame sheet location is reached. Diffusion across stream tubes is ignored. The effect of diffusion is accounted for by the flame sheet shape. The flame sheet ordinates (x_0, y_f) are given by

$$y_f = y_f(x_0) \qquad x_0 \le x_D \tag{1a}$$

$$= w \qquad x_0 > x_D \tag{1b}$$

where w is the width of the semichannel, and x_D is the axial distance required for the flame sheet to reach the channel centerline. Flow velocity, pressure, and temperature are assumed to remain constant. The semichannel is assumed to have a unit height. The model does not represent an exact solution of the equations of motion, even in a limiting sense, but is expected to retain the main features of the diffusion-reaction-lasing process.

Let n_v denote the number density (mol/cm^3) of molecules at vibrational level v. Vibrational levels from $v=0$ to $v=v_f$ are considered. The molecules in each vibrational level are assumed to be in rotational equilibrium at a temperature equal to the local translational temperature T. Only P-branch transitions $(v+1,\ J-1\rightarrow v,\ J)$ are considered. The gain associated with these transitions can be expressed as

$$g_{v,J} = \sigma_{v,J}(n_{v+1} - A_{v,J} n_v) \tag{2a}$$

where

$$A_{v,J} = e^{-2JT_R/T} \tag{2b}$$

The value of $\sigma_{v,J}$ at line center of a Doppler-broadened P-branch transition can be found from[8] (using a corrected numerical coefficient 2.74 $(\ln 2)^{-1/2}$)

$$\sigma_{v,J} = 3.29\times 10^{47}\bar{\sigma} T_R M^{1/2} T^{-3/2} M_{v,J}^2 J e^{-J(J-1)T_R/T} \tag{2c}$$

where, for an HF lasing molecule, $\bar{\sigma}=1$, $T_R = 30.16°$ K, $M = 20$ g/mol,

$$M_{0,J}^2 \times 10^{38} = 0.96[1+0.063J]\text{erg-cm}^3 \tag{2d}$$

$$M_{v,J}^2 / M_{0,J}^2 = 1 + v - 0.01v^3 \tag{2e}$$

$$\sigma_{0,J} = 5.66\times 10^7 (400/T)^{3/2}\text{cm}^2/\text{mol} \tag{2f}$$

Equations (2d) and (2e) are correlations of estimates provided by J. M. Herbelin, which are believed to be accurate to within about 10% for $1 \le J \le 16$ and $v \le 6$.

For convenience, the symbols $g_{v,J}, \sigma_{v,J}$, and $A_{v,J}$ are now denoted g_v, σ_v, and A_v, respectively; i.e., the dependence on J is not displayed. It is assumed that, when lasing occurs, only one transition, with intensity denoted by $\bar{I}_{v,J} \equiv \bar{I}_v$, is permitted between $v+1$ and v. In order to obtain closed-form solutions, vibration-vibration (v-v) collisions are neglected. The rate of change of n_v in each stream tube then can be expressed as

$$\frac{u dn_v}{dx} = u\left(\frac{dn_v}{dx}\right)_p + \left[\left(k_{cd}^{(v+1)} + k_{sp}^{(v+1)}\right) n_{v+1} - \left(k_{cd}^{(v)} + k_{sp}^{(v)}\right) n_v\right] + \left[\left(\frac{\bar{I}g}{\epsilon}\right)_v - \left(\frac{\bar{I}g}{\epsilon}\right)_{v-1}\right] \tag{3}$$

where $u(dn_v/dx)_p$ is the rate (mol/cm^3/sec) of formation of n_v by the chemical "pumping" reaction, as discussed in Appendix A. The second term on the right side of Eq. (3) is the net rate of formation of n_v by collisional deactivation (see Appendix A) and by spontaneous emission. The quantities $k_{cd}^{(v)}$ and $k_{sp}^{(v)}$ are the rates (sec^{-1}) of collisional deactivation and spontaneous emission, respectively, from v to $v-1$ levels. Note that $k_{sp}^{(0)} = k_{cd}^{(0)} = 0$. Generally, $k_{sp}^{(v)}/k_{cd}^{(v)} << 1$ for HF lasers. The last term on the right side of Eq. (3) is the net rate of formation of n_v due to stimulated emission and absorption.

We now introduce the following normalized variables

$$\zeta = x k_{cd}^{(1)}/u \qquad I_v = \sigma_v \bar{I}_v / (\epsilon_v k_{cd}^{(1)})$$

$$N_i = (n_r w)^{-1}\int_0^{y_f} n_i dy \qquad r_v = (k_{cd}^{(v)} + k_{sp}^{(v)})/k_{cd}^{(1)}$$

$$G_v = (\sigma_v n_r w)^{-1}\int_0^{y_f} g_v dy = N_{v+1} - A_v N_v \tag{4}$$

The quantity n_r is a reference number density, which, for a cold-reaction HF laser, is taken to equal $(n_F)_\infty$. Equation (3) is integrated with respect to y, between the limits $y=0$ and $y=y_f$. If it is assumed that r_v is a constant, I_v is a function only of x, i.e., a mean value is used at each station, and $n_v = 0$ at the flame sheet, the result is

$$dN_v/d\zeta + (r_v + I_{v-1} + A_v I_v) N_v - (r_{v+1} + I_v) N_{v+1} - (AIN)_{v-1} = (dN_v/d\zeta)_p \tag{5a}$$

with the boundary condition $N_v(0) = 0$. An alternative form of Eq. (5a) which retains G_v is

$$dN_v/d\zeta - (r_{v+1} N_{v+1} - r_v N_v) - (I_v G_v - I_{v-1} G_{v-1}) = (dN_v/d\zeta)_p \tag{5b}$$

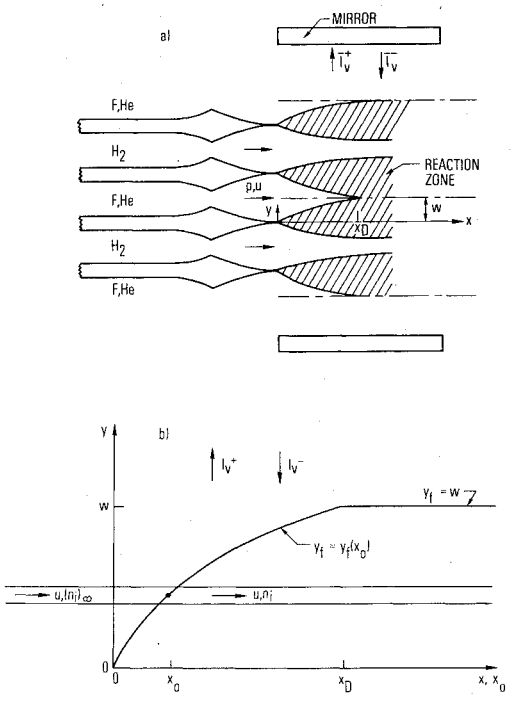

Fig. 1 Mixing model of Mirels, Hofland, and King. Reactants are premixed. Reaction starts at x_0, i.e., at intercept of stream tube with flame sheet $y_f = y_f(x_0)$. $\bar{I}_v = \bar{I}_v^+ + \bar{I}_v^-$. a) typical physical flow; b) corresponding model semichannel flow.

Let

$$N_{ToT} = \sum_{v=0}^{v_f} N_v$$

Since N_{T0T} can be changed only by the pumping process, it follows that

$$\frac{dN_{ToT}}{d\zeta} = \sum_{v=0}^{v_f} \left(\frac{dN_v}{d\zeta}\right)_p \tag{5c}$$

For a cold-reaction HF laser, Eq. (A5),

$$(dN_v/d\zeta)_p = a_v K_I N_F \tag{6a}$$

where

$$K_I N_F = K_I e^{-K_I\zeta} \int_0^\zeta e^{K_I\zeta_0} \frac{dY_0}{d\zeta_0} d\zeta_0 \tag{6b}$$

$$= dY/d\zeta \qquad K_I \to \infty \tag{6c}$$

Here

$$Y_0 = y_f(x_0)/w \qquad Y = y_f(x)/w$$

$$k_p = \sum_{v=0}^{v_f} k_p^{(v)} \qquad a_v = k_p^{(v)}/k$$

$$K_I = k_p/k_{cd}^{(J)} \qquad n_r = (n_F)_\infty$$

In view of the normalizations in Eq. (4), the limit $K_I \to \infty$ in Eq. (6c) corresponds to $k_p \to \infty$. The rate of change of the total N_v population is, from Eqs. (5c) and (6a),

$$dN_{ToT}/d\zeta = K_I N_F \tag{7}$$

Conservation of F atoms yields

$$N_{ToT} + N_F = Y \tag{8}$$

It follows that

$$N_{ToT} = K_I e^{-K_I\zeta} \int_0^\zeta e^{K_I\zeta_0} Y_0 d\zeta_0 \tag{9a}$$

$$= Y \qquad K_I \to \infty \tag{9b}$$

The flame sheet shape can be expressed in the form

$$Y = (\zeta/\zeta_D)^m \qquad Y_0 = (\zeta_0/\zeta_D) \qquad (\zeta \le \zeta_D) \tag{10a}$$

$$Y = 1 \qquad Y_0 = 1 \qquad (\zeta > \zeta_D) \tag{10b}$$

where $m = \frac{1}{2}$ and 1 for laminar and turbulent mixing, respectively.

Now let ϕ_v denote the number of photons emitted up to station ζ, per initial n_r particle, from the transition $v=1$, $J-1 \to v, J$. Thus,

$$\phi_v = (un_r w)^{-1} \int_0^x dx \int_0^{y_f(x)} (g\bar{I}/\epsilon)_v dy \tag{11}$$

$$= \int_0^\zeta I_v G_v d\zeta \tag{12}$$

The quantity $d\phi_v/d\zeta = I_v G_v$ is a measure of the local emitted photon flux per initial n_r particle. Let P denote the net output power, per semichannel, up to station ζ. A semichannel of unit height is assumed. It follows that

$$P = un_r w \sum_{v=0}^{v_f-1} \epsilon_v \phi_v \tag{13}$$

When a mean photon energy ϵ is used, $P = un_r w \epsilon \phi$, where

$$\phi \equiv \sum_{v=0}^{v_f-1} \phi_v$$

is the net photon output per initial n_r particle up to station ζ.

B. Zero-Power and Amplifier Cases

When I_v is specified, Eq. (5a) is linear and generally can be integrated in closed form in order to find N_v as a function of ζ. The net gain per semichannel is then found from $G_v = N_{v+1} - AN_v$.

For the zero-power case ($I_v = 0$), Eq. (5a) yields

$$N_v e^{r_v\zeta} = a_v K_I \int_0^\zeta e^{r_v\zeta} N_F d\zeta + r_{v+1} \int_0^\zeta e^{r_v\zeta} N_{v+1} d\zeta \tag{14}$$

Equation (14) is integrated successively, starting with $v = v_f$. Note that $r_0 = 0$. Expressions for N_v and G_v are given in Appendix B.

It is of interest to expand Eq. (5a) in a power series about $\zeta = 0$. Consider the case $K_I \to \infty$, $Y = (\zeta/\zeta_D)^m$. It is found that

$$N_v/Y = a_v + \zeta(m+1)^{-1}[(r_{v+1} + I_v)a_{v+1} + (AIa)_{v-1} - (r_v + I_{v-1} + A_v I_v)a_v]_{\zeta=0} + O(\zeta^2) \tag{15a}$$

For the zero-power case

$$N_v/Y = a_v + \zeta(m+1)^{-1}[(ra)_{v+1} - (ra)_v] + O(\zeta^2) \tag{15b}$$

The corresponding gain per semichannel is

$$G_v/Y = (a_{v+1} - A_v a_v) + \zeta(m+1)^{-1}\{[(ra)_{v+2} - (ra)_{v+1}] - A_v[(ra)_{v+1} - (ra)_v]\} + O(\zeta^2) \tag{15c}$$

The first term on the right side of Eqs. (15) is the contribution of the pumping reaction, and the second term is the modification because of radiative and collisional deactivation. The pumping reaction increases N_v and G_v by an amount proportional to Y, whereas deactivation increases (or decreases) N_v and G_v by an amount proportional to ζY. Equations (15) are similar in form to the results of Hofland and Mirels,[4,5] where a laminar flame-sheet solution was obtained by expansion about $x=0$.

Zero-power number density and gain distributions for a cold-reaction HF laser, in the limit $K_1 \to \infty$, $Y=(\zeta/\zeta_D)^m$, are given in Fig. 2. For small ζ N_v and G_v vary as Y. In the limit $\zeta \to \infty$, $N_0 \to Y$, and for $v \neq 0$, $N_v \sim \zeta^{m-1}$. The population inversion is total for small ζ and becomes partial with increases in ζ. The gain per semichannel is a maximum at values of ζ of order 1. In interpreting Figs. 2b and 2d, it should be recalled that, in physical variables, the gain per semichannel is proportional to $\sigma_v G_v \sim (v+1)G_v$ for a fixed value of J. Hence, for laminar flow and fixed J, the peak gain on the 2-1 transition is somewhat larger than the peak gain on the corresponding 1-0 transition (Fig. 2b), although this is not true for turbulent flow (Fig. 2d).

The present results are expected to be modified somewhat by vibration-vibration collisions, which are neglected herein. These results are useful however, for providing convenient first estimates of zero-power number density and gain.

C. Oscillator Cases

We now estimate net oscillator output power following a procedure similar to that used by Broadwell[7] and Emanuel and Whittier.[8] A Fabry-Perot optical cavity is assumed. Steady-state lasing is assumed to be initiated simultaneously on all transitions ($v=0,1,2,\ldots,v_f-1$) at some station denoted ζ_i. The value of J is assumed to be the same for each lasing transition, i.e., $A_v=A=\text{const}$. The choice for J is discussed later. All photons are assumed to have the same energy, i.e., $\epsilon_v=\epsilon$.

The condition for steady-state lasing requires that, in the lasing region,[8]

$$\sigma_v G_v = [(-1)\ln(R_1R_2)]/[2n_{sc}n_r w] \quad v<v_f$$
$$\equiv \sigma_0 G_c \tag{16}$$

where R_1 and R_2 are the cavity mirror reflectivities, and n_{sc} is the number of semichannels between the mirrors. The quantity $G_c=\sigma_v G_v/\sigma_0$ denotes the constant value of G_0 in the lasing region. Equation (16) does not apply at $v=v_f$ because there is no lasing from $v_f+1 \to v_f$. For a given optical cavity, laser geometry, and flow conditions, the product $\sigma_0 G_c$ is a constant. However, the individual values of σ_0 and G_c depend on the choice for J. Saturated laser operation corresponds to $G_c \to 0$.

Upstream of ζ_i, $\phi=0$. The variation of ϕ with ζ, downstream of ζ_i, is found as follows. Equation (5b) can be expressed as

$$I_v G_v = dN_v/d\zeta - (dN_v/d\zeta)_p + r_v N_v - r_{v+1}N_{v+1} + I_{v-1}G_{v-1} \tag{17}$$

Successive solutions of Eq. (17) for I_0G_0, I_1G_1, etc., yield

$$I_v G_v = \sum_{i=0}^{v} \left[\frac{dN_i}{d\zeta} - \left(\frac{dN_i}{d\zeta}\right)_p\right] - r_{v+1}N_{v+1} \tag{18}$$

The rate of change of net photon output is, then, after algebraic simplification

$$\frac{d\phi}{d\zeta} \equiv \sum_{v=0}^{v_f-1} I_v G_v = \sum_{v=0}^{v_f} \left[v\left(a_v \frac{dN_{ToT}}{d\zeta} - \frac{dN_v}{d\zeta}\right) - r_v N_v\right] \tag{19}$$

Equation (19) can be deduced more directly by consideration of conservation of vibrational energy; i.e., the rate of change of output power equals the rate of increase of vibrational energy created by the pumping process less the rate of increase of vibrational energy of the N_v particles, less the rate of energy lost by vibration-translation collisions. It is clear that vibration-vibration collisions conserve vibrational energy, and if these had been included in the present study they would not appear in Eq. (19).

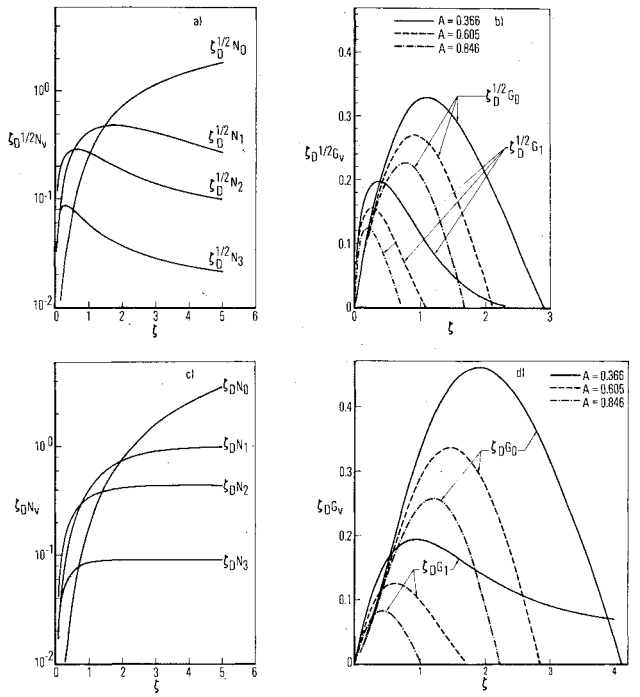

Fig. 2 Zero-power number density and gain distribution for cold-reaction HF laser. $K_1 \to \infty$, $Y=(\zeta/\zeta_D)^m$, $r_v=v$, $v_f=3$, $a_v=0.0, 0.17, 0.55, 0.28$. **a) Number density, $m=\frac{1}{2}$; b) Gain, $m=\frac{1}{2}$; c) Number density, $m=1$, d) Gain, $m=1$.**

We now express N_v in terms of G_0 and N_{ToT}, which are known quantities. Successive solutions of $N_v=G_{v-1}+AN_{v-1}$ for N_1, N_2, etc., indicate

$$N_v = A^{v-1}\sum_{i=0}^{v-1}(G_i/A^i) + A^v N_0 \tag{20}$$

where the summation is taken equal to zero for $v=0$. An expression for N_0 is found by summing Eq. (20) for $v=0, 1,\ldots v_f$. The result is

$$N_0 \sum_{0}^{v_f} A^v = N_{ToT} - \sum_{v=0}^{v_f-1} G_v \sum_{i=0}^{v_f-1-v} A^i \tag{21}$$

Substitution of Eq. (21) into Eq. (20) yields

$$N_v = F_v N_{ToT} + H_v G_c \tag{22}$$

where

$$F_v = A^v \Big/ \sum_{v=0}^{v_f} A^v \tag{23a}$$

$$H_v = A^{v-1}\sum_{i=0}^{v-1}\frac{\sigma_0/\sigma_i}{A^i} - F_v \sum_{v=0}^{v_f-1}\left[\frac{\sigma_0}{\sigma_v}\sum_{i=0}^{v_f-1-v} A^i\right] \tag{23b}$$

Equation (23a) can be expressed as

$$F_v = A^v(A-1)/(A^{v_f+1}-1) \qquad A \neq 1$$
$$= (v_f+1)^{-1} \qquad A=1 \tag{24a}$$

For $\sigma_0/\sigma_v=1$, Eq. (23b) becomes

$$H_v = [A^v(1+v_f)/(A^{v_f+1}-1)] - (A-1)^{-1} \qquad A \neq 1$$
$$= v - (v_f/2) \qquad A=1 \tag{24b}$$

The quantities F_v and H_v are independent of ζ. Also,

$$\sum_{v=0}^{v_f} F_v = 1 \qquad \sum_{v=0}^{v_f} H_v = 0$$

Thus, N_v is known. Substitution of Eq. (22) into Eq. (19) yields

$$d\phi/d\zeta = C_1 dN_{ToT}/d\zeta - C_2 N_{ToT} - C_3 G_c \tag{25a}$$

where it is assumed that $dG_c/d\zeta = 0$ and

$$C_1 = \sum_{v=1}^{v_f} v(a_v - F_v) \quad C_2 = \sum_{v=1}^{v_f} r_v F_v \quad C_3 = \sum_{v=1}^{v_f} r_v H_v$$

If terms of order A compared with one are neglected

$$C_1 = \sum_{1}^{v_f} v a_v \quad C_2 = A \quad C_3 = \sum_{1}^{v_f} r_v (\sigma_0/\sigma_{v-1})$$

The latter equals v_f when $r_v = \sigma_{v-1}/\sigma_0 = v$. From the definition of C_1, it is clear that C_1 equals the number of photons liberated per lasing species molecule (formed by the chemical reaction) for the case of a saturated laser with no collisional deactiviation. Similarly, C_2 is the ratio of the net collisional deactivation rate in a saturated laser to the collisional deactivation rate that would exist if all the lasing species molecules were in the first vibrational level. The quantity $C_3 G_c/N_{ToT}$ is the correction to C_2, i.e., increased collisional deactivation, due to a lack of optical saturation.

Equation (25a) applies downstream of ζ_i. The net photon output, up to station ζ, is

$$\phi = C_1 [N_{ToT}]_{\zeta_i}^{\zeta} - C_2 \int_{\zeta_i}^{\zeta} N_{ToT} d\zeta - C_3 G_c (\zeta - \zeta_i) \tag{25b}$$

The optical cavity is assumed to end at the streamwise station, where $d\phi/d\zeta$ becomes zero or negative. The latter station is denoted ζ_e, and the corresponding net photon output and power output are denoted ϕ_e and P_e, respectively. If ΔH represents the chemical energy released, per mole of n_r particles, the chemical efficiency of the laser is

$$\eta_c \equiv P_e/(n_r u w \Delta H) = (\epsilon/\Delta H)\phi_e \tag{26}$$

where $\epsilon/\Delta H = 1/3$ for a cold-reaction HF laser operating at 2.706 μm. The product 2.327 ϕ_e yields the output at this wavelength in terms of kilojoules per gram of fluorine.

Oscillator performance now can be deduced. Consider the limit $K_1 \to \infty$ with a flame sheet given by $Y = (\zeta/\zeta_D)^m$ for $\zeta < \zeta_D$, and $Y = 1$ for $\zeta > \zeta_D$. Equations (25) yield

$$\zeta^m{}_D (d\phi/d\zeta) = mC_1 \zeta^{m-1} - C_2 \zeta^m - C_3 \zeta^m{}_D G_c \quad (\zeta_i < \zeta < \zeta_D) \tag{27a}$$

$$\frac{\phi_e}{C_1} = \left\{ \left(\frac{\zeta}{\zeta_D}\right)^m - \frac{C_2 \zeta_D}{(m+1)C_1} \left(\frac{\zeta}{\zeta_D}\right)^{m+1} - \left(\frac{C_3 G_c}{C_2}\right)\left(\frac{C_2 \zeta}{C_1}\right) \right\}_{\zeta=\zeta_i}^{\zeta=\zeta_e} \tag{27b}$$

where, for $(C_2\zeta_D/mC_1) \geq [1 + (C_3 G_c/C_2)]^{-1}$,

$$\left(\frac{C_2\zeta_e}{mC_1}\right)^m = \left[1 + \frac{C_2\zeta_D}{2C_1}\left(\frac{C_3 G_c}{C_2}\right)^2\right]^{1/2} - \left(\frac{C_2\zeta_D}{2C_1}\right)^{1/2} \frac{C_3 G_c}{C_2} \qquad (m = 1/2) \tag{28a}$$

$$= 1 - [(C_2\zeta_D/C_1)\ (C_3 G_c/C_2)] \qquad (M = 1) \tag{28b}$$

and, for $(C_2\zeta_D/mC_1) \leq [1 + (C_3 G_c/C_2)]^{-1}$

$$\zeta_e = \zeta_D \tag{28c}$$

Equations (28a) and (28b) are obtained by setting Eq. (27a) equal to zero, and correspond to cases in which lasing terminates before the flame sheet reaches the channel centerline. Equation (28c) corresponds to cases in which lasing is terminated when the flame sheet reaches the channel centerline. The quantity ζ_i can be found from Eq. (16) and the equations given in Appendix B. In most cases, $\zeta_i^2 << 1$, and Eq. (15c) can be expressed

$$\left(\frac{\zeta_i}{\zeta_D}\right)^m = \frac{\sigma_0 G_c}{\sigma_v (a_{v+1} - A a_v)} \left[1 - \frac{\zeta_i}{m+1} \frac{[(ra)_{v+1} - (ra)_{v+2}] - A[(ra)_v (ra)_{v+1}]}{a_{v+1} - A a_v} + O(\zeta_i^2) \right]^{-1} \tag{29}$$

where $\sigma_0 G_c$ is given by Eq. (16). Equation (29) is written in a form that can be solved for ζ_i by iteration with $\zeta_i = 0$ used as the initial estimate. For a given value of J, the value of v that yields the smallest value of ζ_i; i.e., corresponds to the transition with the largest zero power gain, is used. The choice of $v = 1$ (2) appears appropriate for cold-reaction HF(DF) lasers. If no solution for ζ_i is obtained, threshold is not reached.

In most practical devices, the optical medium is saturated, and lasing originates near $\zeta = 0$. In these cases, Eqs. (27) and (28) can be simplified considerably. Assume that $(\zeta_i/\zeta_D)^m \equiv 0(G_c) << 1$, $(C_3 G_c/C_2)^2 << 1$, and $C_2\zeta_D/C_1 = 0$ (1). Equations (27) and (28) become, for $C_2\zeta_D/mC_1 \geq [1 + (C_3 G_c/C_2)]^{-1}$,

$$(m+1)\left(\frac{C_2\zeta_D}{mC_1}\right)^m \frac{\phi_e}{C_1} = 1 - m(m+1)\left(\frac{C_2\zeta_D}{mC_1}\right)^m \frac{C_3 G_c}{C_2} + O(G_c) + O[(\frac{C_3 G_c}{C_2})^2] \tag{30a}$$

$$\left(\frac{C_2\zeta_e}{mC_1}\right)^m = 1 - \left(\frac{mC_2\zeta_D}{C_1}\right)^m \frac{C_3 G_c}{C_2} + O\left(\frac{C_3 G_c}{C_2}\right)^{2(1-m)/m} \tag{30b}$$

and, for $C_2\zeta_D/mC_1 \leq [1 + (C_3 G_c/C_2)]^{-1}$,

$$\frac{\phi_e}{C_1} = 1 - \left(\frac{1}{m+1} + \frac{C_3 G_c}{C_2}\right)\frac{C_2\zeta_D}{C_1} + O(G_c) \tag{30c}$$

$$\zeta_e = \zeta_D \tag{30d}$$

Equations (30) are plotted in Fig. 3 for $m = 1/2$ and define saturated laser performance. The discontinuity in these curves is a result of the neglect of higher-order terms in Eqs. (30).

For a cold-reaction HF laser

$$C_1 = 2.11 - C_2 \tag{31a}$$

$$C_2 = A(1-A)(1+2A+3A^2)/(1-A^4) \tag{31b}$$

and, to within 1%, $C_3 = 3.0 + 1.7A(1-A)$. It is seen that $C_2 \to 0$ as $A \to 0$. This result is explained as follows. Recall that C_2 is the ratio of the collisional deactivation rate in a saturated laser to the collisional deactivation rate that would exist if all the lasing species molecules, i.e., HF, were in the first vibrational level. When $A = 0$ in a saturated laser, stimulated emission reduces all lasing molecules to the ground state. Hence, there is no collisional deactivation in this case, and $C_2 = 0$. This limit can not be achieved in practice because $\sigma_0 \to 0$ as $A \to 0$ such that $G_c \equiv (\sigma_0 G_c)/\sigma_0 \to \infty$ for nonzero values of $\sigma_0 G_c$.

It is assumed that the value of J is the same for all lasing transitions, but the choice for J has not yet been established. In Fig. 4, the effect of J on HF laser output is indicated for

the realistic range of conditions $0 \le \sigma_0 G_c \le 10^5$ cm^2/mole, $0.0 \le \zeta_D \le 20$, and $T = 300°$ and 600° K. For these conditions and small values of J, the optical medium is saturated, and laser output increases with increase in J. With further increase in J, the medium becomes unsaturated because of the decrease in σ_v with increase in J, i.e., Eqs. (2c) and (2f), and laser output reaches a maximum.† Thereafter, an increase in J results in reduced laser output. Further increases in J result in threshold not being reached. Emanuel and Whittier[8] recommended that the value of J that yields the maximum output power be used to estimate laser performance. This approach may tend to overestimate the average value of J and the output power from an actual device. An alternative approach is to use values of J that are observed experimentally. In typical cold-reaction HF and DF lasers, the output power appears to be centered about $J = 5$ to 8 and $J = 8$ to 10 transitions, respectively,[9,10] although these results depend somewhat on initial gas temperatures, degree of dilution, and optical cavity configuration. Hence, the values $J = 7$, 9 appear to be representative experimental values for HF and DF lasers, respectively. Further study concerning the choice for J is desirable.

III. Discussion of Results

The dependent variables are functions of the independent variable ζ; the parameters ζ_D, K_I, G_c, A, J (or T), and m; and lasing molecule distributive properties $(r_v, \sigma_v/\sigma_0, a_v)$. The quantities of ζ, ζ_D, and K_I are the ratios of streamwise distance, characteristic diffusion distance, and characteristic pumping distance to characteristic collision deactivation distance; whereas the quantity G_c is a measure of optical saturation. For zero-power cases with $\zeta \le \zeta_D$, the dependent variables $\zeta_D^m N_v, \zeta_D^m G_v$ are independent of ζ_D. In oscillator cases, the quantities ϕ_e/C_1 and $C_2\zeta_e/C_1$ depend on

$$C_2\zeta_D/C_1,\ C_3G_c/C_2,\ C_1K_1/C_2, \text{ and } C_2\zeta_i/C_1$$

When

$$\zeta_i^2 << 1 \text{ and } C_2\zeta_D/C_1 \ge [1+(C_3G_c/C_2)]^{-1}$$

the quantity

$$(C_2\zeta_D/C_1)^m \phi_e/C_1$$

is a function only of

$$(C_2\zeta_D/C_1)^m (C_3G_c/C_2) \text{ and } C_1K_1/C_2$$

In practical lasers, the assumptions incorporated in Eq. (30) are approximately valid. The resulting variation of efficiency and output power with $C_2\zeta_D/mC_1$ and $(C_2\zeta_D/mC_1)^{1/2}(C_3G_c(C_2)$ is shown in Fig. 3 for $m = 1/2$. Note that $(C_2\zeta_D/mC_1)^{1/2}(C_3G_c/C_2)$ is independent of pw. For small values of ζ_D, the flow corresponds to that for a premixed laser. In Fig. 3a, it is indicated that laser efficiency decreases as ζ_D increases. The ordinate in Fig. 3b is proportional to output power per semichannel when plenum temperatures and a stoichiometry (p_F/p) are kept constant. It is shown that output power increases with ζ_D until $C_2\zeta_D/mC_1 = [1+(C_3G_c/C_2)]^{-1}$ and remains constant with further increases in ζ_D. In the latter region, lasing is terminated before the fuel (H_2) reaches the centerline of the oxidizer (F) channel.

The present results can be expressed readily in terms of physical variables. First consider a cold-reaction HF laser with combustor-generated DF present in the oxidizer flow. Let p_F and p_{DF} denote the initial partial pressures of atomic fluorine and DF, respectively, and let p_F characterize the mean value of p_{HF} in the reaction zone. Assume that HF and DF are the major deactivators of HF(v), and use only the

†The maxima in Fig. 4 are predicted to within a few percent by using $\zeta_i = 0$ in Eq. (27b).

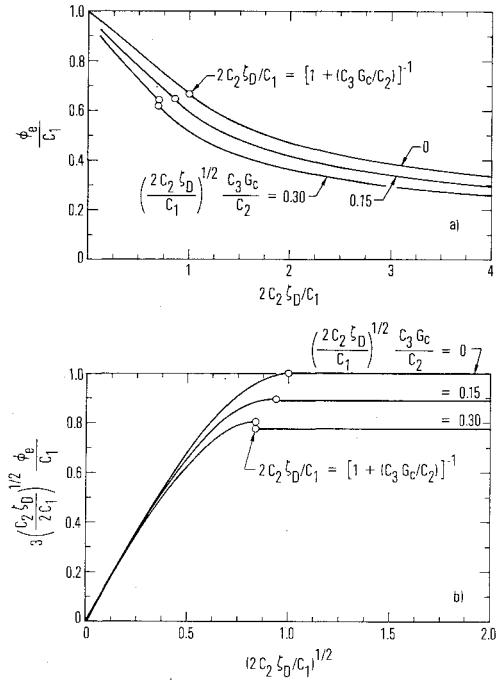

Fig. 3 Saturated laser performance for $K_I \to \infty$ and $m = 1/2$, [Eqs. (30)]. a) Efficiency; b) Output power.

leading terms in Eqs. (A9) and (A10). Recall that $\zeta = k_{cd}^{(1)} x/u$. It follows that

$$\zeta = \frac{0.0752p(\text{Torr})x(\text{cm})}{(p/p_F)(T/400)^2}\left(\frac{4\times10^5}{u}\right)[1+0.6(\frac{p_{DF}}{p_F})] \tag{32}$$

Characterize laminar and turbulent flame shapes by $y_f^L = A_L(\mathfrak{D}x/u)^{1/2}$ and $y_f^T = A_T x$, respectively, where $A_L = 0(1)$, $A_T = 0(0.1)$, and $\mathfrak{D} = CT^{3/2}/p$ is the laminar diffusion coefficient. Then, $x_D^L = (w/A_L)^2 u/\mathfrak{D}, x_D^T = w/A_T$, and the corresponding laminar and turbulent values of ζ_D^m are

$$(\zeta_D^L)^{1/2} = \frac{2.072p(\text{Torr})w(\text{cm})}{(p/p_F)^{1/2}(T/400)^{7/4}}\left(\frac{2.88\times10^{-4}}{C}\right)^{1/2}$$

$$\left(\frac{2}{A_L}\right)[1+0.6(\frac{p_{DF}}{p_F})]^{1/2} \tag{33a}$$

where $C = 2.88\times10^{-4}$ corresponds to the diffusion of hydrogen into helium and

$$\zeta_D^T = \frac{0.752p(\text{Torr})w(\text{cm})}{(p/p_F)(T/400)^2}\frac{4\times10^5}{u}\frac{0.1}{A_T}[1+0.6(\frac{p_{DF}}{p_F})] \tag{33b}$$

Similarly, if we let $\sigma_0 = \sigma_{0,J}$ and $n_r = p_F/RT$, Eq. (16) becomes, for a HF lasing molecule,

$$G_c = \frac{0.234(p/p_F)(T/400)^{5/2}\ln(R_1R_2)^{-1}}{n_{sc}p(\text{Torr})w(\text{cm})}$$

$$\frac{\exp[J(J-1)T_R/T]}{J(1+0.063J)} \tag{33c}$$

where $\sigma_{0,J}$ has been evaluated from Eqs. (2). Note that $\zeta_D^m G_c$ is independent of pw. Recall that $C_1 = 2.11$, $C_3 = 3$, and $C_2 = \exp(-2JT_R/T)$ for a HF laser with $C_2 << 1$. Hence, the dependence of laser performance on physical variables can be readily deduced, e.g., Fig. 3 and Eqs. (33).

Now note explicit expressions for ϕ_e and ζ_e for a saturated laser ($G_c = 0$) in the limit $K_I \to \infty$, $C_2\zeta_D/mC_1 > 1$. From Eqs. (30) and (33)

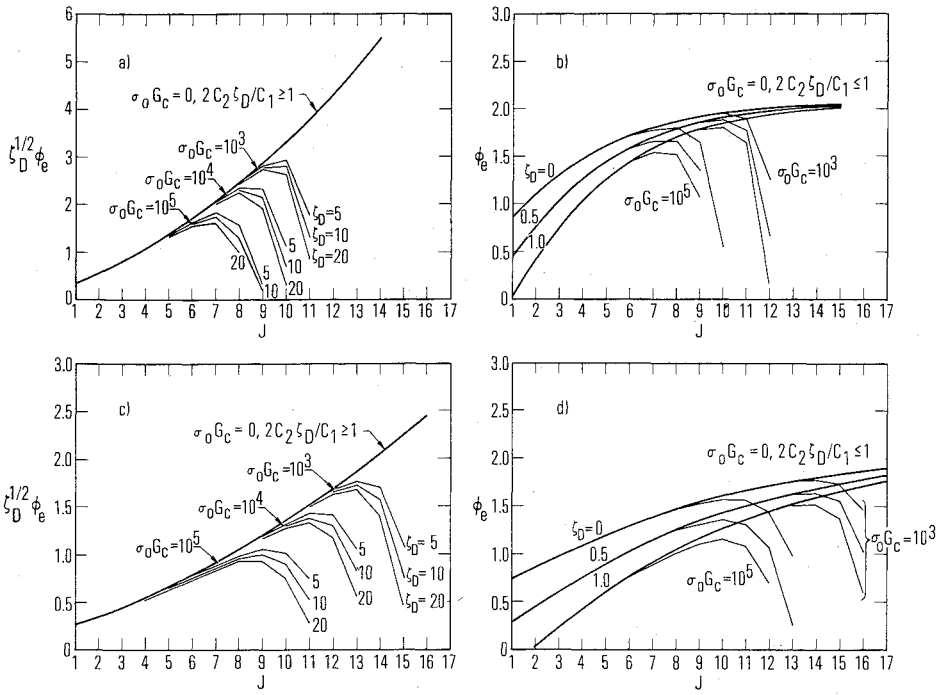

Fig. 4 Effect of J variation on output power from cold-reaction HF chemical laser. $K_1 \to \infty$, $m = \frac{1}{2}$, $r_v = v$, $\sigma_v/\sigma_0 = v+1, a_v = 0.0, 0.17, 0.55, 0.28, \sigma_0 G_c =$ cm^2/mol. **a)** $T = 300$ K, $5 \leq \zeta_D \leq 20$; **b)** $T = 300$ K, $0 \leq \zeta_D \leq 1$, **c)** $T = 600$ K, $5 \leq \zeta_D \leq 20$; **d)** $T = 600$ K, $0 \leq \zeta_D \leq 1$.

$$\phi_e = 0.228 \frac{C_1^{3/2}}{C_2^{1/2}} \frac{(p/p_F)^{1/2}(T/400)^{7/4}(C/2.88\times10^{-4})^{1/2}(A_L/2)}{p(\text{Torr})\,w(\text{cm})[1+(0.6p_{DF}/p_F)]^{1/2}} \tag{34a}$$

when m = ½ and

$$\phi_e = 0.665 \frac{C_1^2}{C_2} \frac{(p/p_F)(T/400)^2(u/4\times10^5)(A_T/0.1)}{p(\text{Torr})\,w(\text{cm})[1+(0.6p_{DF}/p_F)]} \tag{34b}$$

when $m = 1$. The dependence of ϕ_e on physical variables is considerably different for the laminar and turbulent mixing cases, except for the dependence on pw. The corresponding length of the lasing zone is, from Eqs. (30b) and (32),

$$x_e(\text{cm}) = \frac{mC_1}{C_2} \frac{(p/p_F)(T/400)^2}{0.0752p(\text{Torr})} \frac{u/4\times10^5}{[1+(0.6p_{DF}/p_F)]} \tag{35}$$

The lasing length is proportional to u/p, which is expected from binary scaling considerations, and is independent of w.

Similar expressions can be deduced for a cold-reaction DF laser with combustor-generated HF present in the oxidizer flow. For a DF lasing molecule, $\bar{\sigma} = 1$, $T_R = 15.6°$ K, $M = 21$ g/mol, and

$$M_{0,J}^2 \times 10^{38} = 0.662[1+0.045J]\text{erg-cm}^3 \tag{36a}$$

$$M_{v,J}^2/M_{0,J}^2 = 1+v-0.005v^3 \tag{36b}$$

$$\sigma_{0,1} = 2.03\times10^7(400/T)^{3/2}\text{cm}^2/\text{mol} \tag{36c}$$

Equations (36) are correlations of estimates by Herbelin that are believed to be accurate to within about 10% for $1 \leq J \leq 13$, $v \leq 6$. Consider HF and DF to be the major deactivators of DF(v), approximate p_{DF} by the initial value of p_F, and include only the leading terms in Eqs. (A10) and (A11). Equations (32-35) then apply for the cold-reaction DF laser if $[1+0.6(p_{DF}/p_F)]$ is replaced by $0.4[1+1.6(p_{HF}/p_F)]$, if $[1+0.063J]$ is replaced by $0.365\ [1+0.045J]$, and if $C = 2.35\times10^{-4}$ (corresponding to diffusion of D_2 into He) is used in Eq. (34a). For a cold-reaction DF laser, $a_v = 0$, 0.10, 0.24, 0.38, and 0.28; hence, $C_1 = 2.84$ and $C_3 = 4$ for $C_2 = \exp(-2JT_R/T) \ll 1$. The product $1.641\ \phi_e$ yields the laser output in terms of kilojoules per gram of fluorine for a mean output wave length of 3.837 μm.

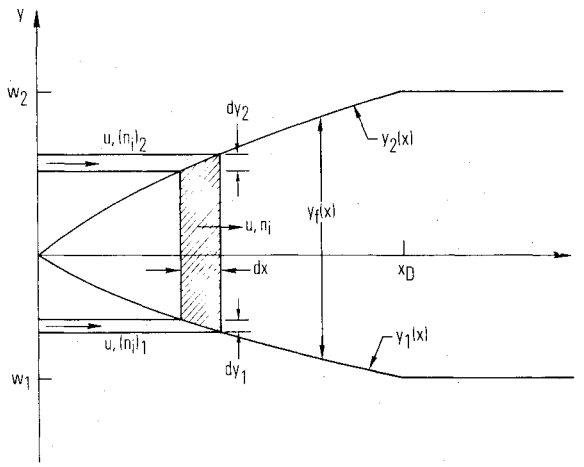

Fig. 5 Mixing model of Broadwell.

The two-level model of Mirels, Hofland, and King[6] corresponds to the choice $v_f = a_l = r_l = A = \sigma_0/\sigma_l = 1$. For this case, $C_1 = C_2 = C_3 = \frac{1}{2}$, and the present results agree with those of Ref. 6‡ For a given lasing species, scaling laws deduced from the multiple-level model differ from those deduced from the two-level model only in the dependence of C_1, C_2, and C_3 on T and J. The effect of the latter on laser performance is approximated, in the two-level model, by appropriate normalizations; e.g., chemical efficiency for $\zeta_D \neq 0$ is normalized to the value for $\zeta_D = 0$, and by the use of suitable mean rates; e.g., $k_{cd}^{(2)}$ was used to characterize HF collisional deactivation.

The mixing model used by Broadwell[7] is illustrated in Fig. 5. It is shown in Appendix C that the latter leads to results that are identical with the flame-sheet-mixing model used herein if mean chemical rate are used in both models.

‡The present oscillator solution becomes identical with the solution of Ref. 6 if the present variables $C_2\zeta/C_1, \phi_e/C_1, C_3G_c/C_2$, and C_1K_1/C_2 are identified with the variables $\zeta, \eta, G_c/\sigma w[F]_o$, and K_1 in Ref. 6.

IV. Concluding Remarks

It is clear from Eqs. (34) that the dependence of ϕ_e on physical variables is different for laminar and turbulent flows. Criteria for determining whether or not the mixing in the lasing region is laminar, transitional, or turbulent have not been established. Incompressible hydrodynamic stability studies indicate that the critical Reynolds number for the mixing of two parallel streams is about a factor of 10 lower than the corresponding value for a semi-infinite flat plate.[11] Flat-plate transition Reynolds numbers vary from values of the order of 10^5 to 10^6 for subsonic flows to values of the order of 10^7 to 10^8 for hypersonic flows. Transition Reynolds numbers for the mixing of parallel streams might be expected to be about one or two orders of magnitude lower than the corresponding flat plate values. The Reynolds number per unit length at the oxidizer nozzle exit for a typical current laser design[12] is of the order of $Re/cm = 0(10^3)$, e.g., helium at $p = 5$ Torr, $T = 300°$ K, $u = 4 \times 10^5$ cm/sec. Most of the laser energy is extracted within a few centimeters of the nozzle exit[12]; hence, the Reynolds number based on the length of the lasing region is of the order of 10^3. The flow external to the mixing zone is hypersonic. This suggests that the mixing is laminar in the region of interest as was, in fact, observed by Varwig[13] and Shackleford et al.[14] Since the lasing length varies as p^{-1} [Eq. (35)] and Re/cm varies as p, the Reynolds number based on lasing length is independent of pressure level, and an increase in pressure level does not result in turbulent mixing in the lasing region. The initial nozzle boundary layer, shock-induced separation at the nozzle exit, and blunt nozzle trailing edges may hasten transition to turbulence.[13] In the latter case, the mixing in the lasing region may be transitional. In these cases, the choice $m = ½$ or an alternative choice for $y_f = y_f(x)$ may be more appropriate than the choice $m = 1$, which implies fully developed turbulent flow. Further study is needed.

It also should be noted that the simplified models of Mirels, Hofland, and King,[6] Broadwell,[7] and the present study neglect features of the flow that may be important in some cases. In particular, initial flow nonuniformity (because of nozzle wall boundary layer); pressure nonuniformity, i.e., shocks, edge effects, and lateral gas expansion; and heat addition effects, i.e., streamwise temperature variation effect on rates are neglected. Appropriate mean values are needed.

Appendix A: Reaction Model

The simplified reaction model used in this report is illustrated by considering pumping and collisional deactivation reactions for a cold-reaction HF laser. Backward reactions are neglected.

A. Pumping Reaction

The cold-reaction HF laser uses molecular hydrogen and atomic fluorine. Vibrationally excited HF is generated by the pumping reaction

$$F + H_2 \xrightarrow{\bar{k}_p^{(v)}} HF(v) + H \tag{A1}$$

where $\bar{k}_p^{(v)}$ is the rate coefficient for production of $HF(v)$, and

$$\bar{k}_p = \sum_{v=0}^{v_f} \bar{k}_p^{(v)}$$

is the overall rate coefficient. The rate of change of n_F along a single stream tube with velocity u, assuming a hydrogen rich mixture, is

$$u dn_F/dx = -\bar{k}_p n_{H_2} n_F \tag{A2a}$$

$$\equiv -k_p n_F \tag{A2b}$$

The quantity $k_p \equiv \bar{k}_p n_{H_2}$ has the units $\sec^{-1}$, and a mean value is used. The reciprocal of k_p is the characteristic pumping time. If the reaction starts at x_0 with an initial concentration $(n_F)_\infty$ (Fig. 1), the downstream concentration of atomic fluorine along the stream tube is

$$n_F/n_F)_\infty = e^{K_p(x-x_0)/u} \tag{A3}$$

Let $a_v = k_p^{(v)}/k_p$ and note

$$\sum_{v=0}^{v_f} a_v = 1$$

From Eqs. (A1) and (A2), the vibrationally excited HF created by the pumping reaction is, for each stream tube,

$$u(dn_v/dx)_p = a_v k_p n_F \tag{A4}$$

The net rate of creation of HF (v) at a given streamwise station, due to all the stream tubes, is found by integrating Eq. (A4) between $y = 0$ and $y_f(x)$. The result, after introduction of nondimensional variables, is

$$(dN_v/d\zeta)_p = a_v K_1 N_F \tag{A5a}$$

where

$$K_1 N_F = K_1 e^{-K_1\zeta} \int_0^\zeta e^{K_1\zeta_0} (dY_0/d\zeta_0)\, d\zeta_0 \tag{A5b}$$

$$= dY/d_\zeta \qquad (K_1 \to \infty) \tag{A5c}$$

and $n_r = (n_F)_\infty$, $Y_0 = y_f(x_0)/w$, $Y = y_f(x)/w$.

B. Collisional Deactivation

Now consider vibration-translation (v-t) deactivation of excited species and neglect vibration-vibration transfer. The v-t deactivation of n_v by species n_i, namely,

$$n_v + n_i \xrightarrow{(\bar{k}_{cd}^{(v)})_i} n_{v-1} + n_i$$

is found from

$$u\, d\, n_v/dx = (\bar{k}_{cd}^{(v)})_i n_i n_v \tag{A6}$$

The deactivation of n_v by all species can be expressed

$$u\, d\, n_v/dx = k_{cd}^{(v)}\, n_v \tag{A7a}$$

where

$$k_{cd}^{(v)} = \sum_i \left(\bar{k}_{cd}^{(v)}\right)_i n_i \tag{A7b}$$

and $k_{cd}^{(o)} = 0$. The quantity $k_{cd}^{(v)}$ is assumed to be a constant, and characteristic values of the major deactivators are used in Eq. (A7b). For arc-driven cold-reaction HF lasers,[10] the major deactivator is HF (and possibly H, F). The number density of each of the latter can be characterized by $(n_F)_\infty$. For combustion-driven HF lasers,[10] the introduction of major deactivation species by the combustor, e.g., DF, needs to be considered.

C. Rate Coefficients

Pumping and collisional deactivation rates for an HF laser, from Cohen,[15] are repeated here for convenience. Units are $T = °$K and $\bar{k} = \text{cm}^3/\text{mol-sec}$. The overall pumping reaction rate is

$$\bar{k}_p = 1.6 \times 10^{14} e^{-805/T} \tag{A8a}$$

and the distributional coefficients are

$$a_v = 0, 0.17, 0.55, 0.28 \qquad (v = 0,1,2,3) \qquad \text{(A8b)}$$

The major collisional deactivation process in arc-driven lasers is

$$HF(v) + HF \rightarrow HF(v-1) + HF$$

for which the rate coefficient is

$$\left(\bar{k}_{cd}^{(v)}\right)_{HF}^{HF^*} = v(3\times 10^{14} T^{-1} + 3.5\times 10^{4} T^{2.26}) \qquad \text{(A9)}$$

The latter differs somewhat from the rate used by Mirels, Hofland, and King.[6] Collisional deactivation of HF(v) by DF, in combustion-driven lasers, can be estimated from[16]

$$\left(\bar{k}_{cd}^{(v)}\right)_{DF}^{HF^*} = v(1.9\times 10^{14} T^{-1} + 1.35\times 10^{2} T^{3}) \qquad \text{(A10)}$$

Equation (A10) neglects vibration-vibration collisions, which may be significant.

The rate coefficient for the collisional deactivation of DF(v) by DF is

$$\left(\bar{k}_{cd}^{(v)}\right)_{DF}^{DF^*} = v(1.2\times 10^{14} T^{-1} + 1.4\times 10^{2} T^{2.96}) \qquad \text{(A11)}$$

The rate coefficient for the deactivation of DF(v) by HF is the same as that indicated in Eq. (A10).

Appendix B: Zero-Power Number Density Distribution

Number density distributions, in the absence of radiation, are found herein for the case $Y = (\zeta/\zeta_D)^m, K_1 \rightarrow \infty, r_v = v$, and $v_f \leq 3$. Integration of Eq. (14) yields the following results.

A. Laminar Flow ($m = 1/2$)

$$\zeta_D^{1/2} N_3 = 3^{-1/2} a_3 D[(3\zeta)^{1/2}] \qquad \text{(B1a)}$$

$$\zeta_D^{1/2} N_2 = 2^{-1/2}(a_2 + 3a_3) D[(2\zeta)^{1/2}] - 3^{1/2} a_3 D[(3\zeta)^{1/2}] \qquad \text{(B1b)}$$

$$\zeta_D^{1/2} N_1 = (a_1 + 2a_2 + 3a_3) D[\zeta^{1/2}] - 2^{1/2}(a_2 + 3a_3) D[(2\zeta)^{1/2}] + 3^{1/2} a_3 D[(3\zeta)^{1/2}] \qquad \text{(B1c)}$$

$$\zeta_D^{1/2} N_0 = \zeta^{1/2} - \zeta_D^{1/2}(N_1 + N_2 + N_3) \qquad \text{(B1d)}$$

where $D[z]$ is the Dawson integral[7]

$$D[z] = e^{-z^2} \int_0^z e^{z_0^2} dz_0$$

$$= z[1 - (2/3)z^2 + 0(z^4)]$$

$$= (2z)^{-1}[1 + (2z^2)^{-1} + 0(z^{-4})] \qquad \text{(B1e)}$$

B. Turbulent Flow ($m = 1$)

$$3\zeta_D N_3 = a_3(1 - e^{-3\zeta}) \qquad \text{(B2a)}$$

$$2\zeta_D N_2 = a_2 + a_3 - (a_2 + 3a_3) e^{-2\zeta} + 2a_3 e^{-3\zeta} \qquad \text{(B2b)}$$

$$\zeta_D N_1 = a_1 + a_2 + a_3 - (a_1 + 2a_2 + 3a_3) e^{-\zeta} + (a_2 + 3a_3) e^{-2\zeta} - a_3 e^{-3\zeta} \qquad \text{(B2c)}$$

$$\zeta_D N_0 = \zeta - \zeta_D (N_1 + N_2 + N_3) \qquad \text{(B2d)}$$

Appendix C: Mixing Models

It is now shown that, when mean values of reaction rates are used, the scheduled-mixing model of Broadwell[7] is equivalent to the mixing model of Mirels, Hofland, and King[6] used herein. The mixing model of Broadwell is illustrated in Fig. 5. For an HF laser, the quantities w_1 and w_2 represent the semichannel widths of the hydrogen and the fluorine-diluent streams, respectively. Both streams have the same velocity u. The reaction zone is assumed to be bounded by two similarly shaped curves, denoted by y_1 and y_2 in Fig. 5. Fluid properties in the reaction zone depend only on x. Freestream particles that intercept the bounding curves between station x and station $x+\Delta x$ are assumed to be uniformly distributed throughout the reaction zone. The axial distance required for all the reactants to enter the reaction zone is denoted by x_D and is equivalent to the diffusion distance in the flame sheet model. Note that w_1 and w_2 are the values of y_1 and y_2 at x_D. Although Broadwell considered only turbulent mixing with $w_1 = w_2$, the author only requires that y_1 and y_2 be similar in shape, i.e., $y_1/y_2 = \text{const}$. Introduce $y_f = y_2 - y_1$. The rate of change of any species n_i in the reaction zone can be expressed as

$$u\frac{dn_i}{dx} = [(n_i)_2 \frac{dy_2}{dy_f} - (n_i)_1 \frac{dy_1}{dy_f}]\frac{u}{y_f}\frac{dy_f}{dx} - \frac{n_i u}{y_f}\frac{dy_f}{dx} + \omega_i \qquad \text{(C1)}$$

where $(n_i)_1$ and $(n_i)_2$ represent the freestream values of n_i intercepting curves y_1 and y_2, respectively. The first term on the right side of Eq. (C1) represents the rate of increase of n_i because of particles entering the reaction zone; the second term represents the decrease in n_i because of the lateral expansion of the reaction zone; the third term represents the rate of change of n_i because of chemical and radiative reactions. Since y_1 and y_2 are assumed to be similar in shape, a mean freestream value of n_i, denoted $(n_i)_\infty$, can be introduced such that

$$(n_i)_\infty = [(n_i)_2 y_2 - (n_i)_1 y_1]/y_f \qquad \text{(C2)}$$

Equation (C1) can then be written as

$$\frac{u}{y_f}\frac{d\{[n_i - (n_i)_\infty]y_f\}}{dx} = \omega_i \qquad \text{(C3)}$$

For lasing molecules, the right side of Eq. (C3) has the same terms as the right side of Eq. (3). Introduce $w = w_2 - w_1, N_v = n_v y_f / w n_r, G_v = g_v y_f / \sigma_v w n_r$, and note $(n_v)_\infty = 0$. Equation (C3) then reduces to Eqs. (5). The term $(dN_v/d\zeta)_p$ in Eqs. (5) is found by integrating Eq. (C3) for $n_i = n_F$. The results are the same as those deduced in Appendix A.

Thus, the mixing model of Broadwell[7] corresponds to a flame sheet model with premixed reactants [the number density being given by Eq. (C2)], a flame sheet location $y_f = y_2 - y_1$, and a diffusion distance x_D, which is evaluated by consideration of the actual diffusion process. At each axial station, number densities in the Broadwell model correspond to average values in the flame-sheet model. The equivalence requires that the coefficients of n_v, in Eq. (3), be independent of y. Hence, the use of mean rates, at each axial station, is required in the flame-sheet model for equivalence.

References

[1] King, W. S. and Mirels, H., "Numerical Study of a Diffusion Type Chemical Laser," *AIAA Journal*, Vol. 10, Dec. 1972, pp. 1647-1654.

[2] Thoenes, J., et. al., "Chemical Laser Analysis Development, Vol. 1, Laser and Mixing Program Theory and Users Guide," TR RK-CR-73-2, Oct. 73, Lockheed Missiles and Space Co., Huntsville, Ala.

[3] Tripodi, R., et al. "A Coupled Two-Dimensional Computer Analysis of CW Chemical Mixing Lasers," AIAA Paper 74-224, 1974.

[4]Hofland, R. and Mirels, H., "Flame Sheet Analysis of CW Diffusion Type Chemical Laser, I. Uncoupled Radiation," *AIAA Journal*, Vol. 10, April 1972, pp. 420-428.

[5]Hofland, R. and Mirels, H., "Flame Sheet Analysis of CW Diffusion Type Chemical Laser, II. Coupled Radiation," *AIAA Journal*, Vol. 10, Oct. 1972, pp. 1271-1280.

[6]Mirels, H., Hofland, R., and King, W. S., "Simplified Model of CW Diffusion Type Chemical Laser," *AIAA Journal*, Vol. 11, Feb. 1973, pp. 156-164.

[7]Broadwell, J. E., "Effect of Mixing Rate on HF Chemical Laser Performance," *Applied Optics*, Vol. 13, April 1974, pp. 962-967.

[8]Emanuel, G. and Whittier, J. S., "Closed Form Solution to Rate Equations for an $F+H_2$ Laser Oscillator," *Applied Optics*, Vol. 11, Sept. 1972, pp. 2047-2056.

[9]Kwok, M. A., Giedt, R. R., and Gross, R. W. F., "Comparison of HF and DF Continuous Chemical Lasers: II. Spectroscopy," *Applied Physics Letters*, Vol. 16, May 15, 1970, pp. 386-387.

[10]Warren, W. R., Jr., "Chemical Lasers," *Aeronautics and Astronautics*, Vol. 13, April 1975, pp. 36-49.

[11]Lin, C. C., *The Theory of Hydrodynamic Stability*, Cambridge University Press, Cambridge, England, 1955, p. 101.

[12]Spencer, D. J., Mirels, H., and Durran, D. A., "Performance of CW HF Chemical Laser With N_2 or He Diluent," *Journal of Applied Physics*, Vol. 43, March 1972, pp. 1151-1157.

[13]Varwig, R. L., "Photographic Observation of CW HF Chemical Laser Reacting Flowfield," *AIAA Journal*, Vol. 12, Oct. 1974, pp. 1448-1450.

[14]Shackleford, W. L., et. al., "Experimental Measurements in Supersonic Reacting $F+H_2$ Mixing Layers," *AIAA Journal*, Vol. 12, Aug. 1974, pp. 1009-1010.

[15]Cohen, N., "A Review of Rate Coefficients for Reactions in the H_2-F_2 Laser System," The Aerospace Corp., El Segundo, Calif., TR-0173(3430)-9, Nov. 1972.

[16]Cohen, N., The Aerospace Corporation, private communication.

[17]Abromowitz, M. and Stegun, I. A., "Handbook of Mathematical Functions," National Bureau of Standards, AMS 55, June 1964, p. 319.